

On the high accuracy lattice parameters determination by n-beam diffraction: Theory and application to the InAs quantum dots grown over GaAs(001) substrate system

L.H. Avanci,^{1,*} C.M.R. Remédios,^{2,†} A.A. Quivy,^{1,‡} and S.L. Morelhão^{1,§}

¹*Instituto de Física, Universidade de São Paulo, CP 66318, 05315-970 São Paulo, SP, Brazil*

²*Departamento de Física, Universidade Federal do Ceará, Campus do Pici, CP 6030, 60455-760, Fortaleza, CE, Brazil*

(Dated: May 1, 2019)

Ultra-precise lattice parameter measurements in single crystals are achievable, in principle, by X-ray multiple diffraction (XMD) experiments. Tiny sample misalignments have hindered the systematic usage of XMD in studies where accuracy is an important issue. In this work, theoretical basement and methods for correcting general misalignment errors are presented. As a practical demonstration, the induced strain of buried InAs quantum dots grown on GaAs (001) substrates is determined. Such a demonstration confirms the possibility to investigate epitaxial nanostructures via the strain field that they generate in the substrate crystalline lattice.

PACS numbers: 61.10.Nz; 61.10.Dp

Keywords: X-ray diffraction, semiconductors, nanomaterials

I. INTRODUCTION

For decades, X-ray multiple diffraction (XMD) phenomenon has been applied in material science for studying a broad range of subjects: in-plane crystalline perfection of surfaces and interfaces^{1,2}; strain determination in single crystals caused by an external stimulus^{3–6}; the studies of habit modification of crystals due to the introduction of impurities species⁷; direct observation of crystallographic phase transition in single crystals⁸; physical measurements of the invariant phase triplets^{9–13}; two-dimensional materials¹⁴ or quasi-crystals^{15,16} and even in the plasma studies and diagnostics^{17,18}.

Among the reasons behind the success of the XMD in material science, one comes from the fact that XMD is the unique technique capable of providing information over several different directions within a crystalline lattice under the same diffraction geometry, *i.e.* with incidence ω and detector 2θ fixed angles. Azimuthally scanning a chosen reflection, also known as Renninger scanning, allows accurate unit-cell lattice-parameters determination. This information is very important for characterizing single crystals under extreme conditions, where the instrumental setup, crystal shape and/or limited choice of X-ray photon energies do not leave too many accessible reflections to be measured. For a clear example, in applying uniform-uniaxial electric fields, electric contacts have to be set on two crystal faces. The field effects over the three-dimensional lattice can be studied by Renninger scanning a reflection that has not been hindered by the contacts³. Exploitation of the synchrotron radiation linear polarization to tune the relative strength of the multiple diffracted waves has significantly increased the number of suitable reflections to be taken for Renninger scanning¹⁹. Moreover, it is also well known that this technique is the most accurate method for experimental lattice parameters measurements in single crystals^{20,21}; the precision can easily

achieve $1/10000\text{\AA}$, depending on the chosen XMD case.

High-precision lattice parameter measurements, absolute or relative (variational), are necessary in several research fields, such as determination of piezoelectric tensor, structural phase transition and doping with low concentrations of impurities (typically parts per million) where the effects produced over the unit cell are very small. In studies where precise lattice parameter measurements are desired, it is essential to account for all possible systematic errors in the Renninger scanning. A source of significant systematic errors originates from the misalignment between the azimuthal rotation axis ϕ -axis and the diffraction vector of the reflection to be scanned, named the primary reflection. Even in very good equipments and careful sample alignment procedures, residual tiny misalignments are always present. Since, in general, these misalignments can be smaller than 0.01° , they have been neglected so far and no further efforts were made to take them into account. However, as experimentally observed, even such small misalignment severely compromise the accuracy of the results. In this article, we present the theory to account for a general sample misalignments as well as the experimental procedure for correcting systematic errors in lattice-parameter measurements by Renninger scanning.

II. THEORY

To excite multiple X-ray diffraction in crystals, the incident beam direction, wavevector \mathbf{k} , must fulfill two conditions summarized by

$$\mathbf{k} \cdot \mathbf{P} = -\mathbf{P} \cdot \mathbf{P}/2 \quad (1)$$

and

$$\mathbf{k} \cdot \mathbf{S} = -\mathbf{S} \cdot \mathbf{S}/2. \quad (2)$$

\mathbf{P} and \mathbf{S} are the diffraction vectors of the primary and secondary reflections, respectively. Equations (1) and (2) stand for the Bragg cones of these reflections in the reciprocal space. In Renninger scanning, the primary reflection is kept excited, *i.e.* Eq. (1) is fulfilled, while the crystal rotates around \mathbf{P} ; it means that the incident beam is parallel to the primary Bragg cone during the azimuthal crystal rotation. The XMD occurs when the secondary reflection is excited by the azimuthal rotation and therefore Eq. (2) is also fulfilled. Note that more than one secondary reflection can be excited (3, 4,... beam cases) at the same azimuthal position; Eq. (2) is valid for all simultaneously diffracting secondary reflections.

The most well-known expressions for determining XMD positions in Renninger scans were obtained from Eq. (2)^{22,23} assuming that the primary reflection is always aligned, *i.e.* Eq. (1) is fulfilled for a complete 360° rotation around \mathbf{P} . However, it is not feasible to account for sample misalignments using the above couple of equations. The reason is that Eq. (1) is not sensitive to misalignments out of the incidence plane of the primary reflection; in other words, when the misalignment between \mathbf{P} and the azimuthal rotation axis (ϕ axis) is taken into account by Eq. (1), it appears in Eq. (2) as a negligible second-order correction. Therefore, a third equation where the sensitivity to the three-dimensional misalignment of \mathbf{P} is the same as in Eq. (2) is necessary. Note that at least two equations are required since the XMD condition depends on the incidence ω and azimuthal ϕ angles *i.e.* depends on two variables.

A third equation that is also fulfilled under XMD condition stands for the Bragg cone of the coupling reflection, whose diffraction vector is given by \mathbf{C} . Since $\mathbf{P} = \mathbf{S} + \mathbf{C}$, it is possible to replace \mathbf{P} by $\mathbf{S} + \mathbf{C}$ in Eq. (1) to obtain

$$\mathbf{k} \cdot \mathbf{C} = -\mathbf{C} \cdot \mathbf{C}/2 - \mathbf{C} \cdot \mathbf{S}. \quad (3)$$

In this equation, the $\Delta\omega$ and $\Delta\phi$ deviations of the incident beam direction $\mathbf{k}(\omega, \phi)$ have now about the same weight that they have in Eq. (2); it leads to a trivial system of linear equations for determining both deviations as a function of the sample misalignment. The dependence of the incident beam direction on these angular deviations can be taken into account by

$$\mathbf{k} \simeq \mathbf{k}_0 + \Delta\omega \mathbf{k}_\omega + \Delta\phi \mathbf{k}_\phi \quad (4)$$

where $\mathbf{k}_\omega = \partial\mathbf{k}/\partial\omega$ and $\mathbf{k}_\phi = \partial\mathbf{k}/\partial\phi$ are calculated at ω_0 and ϕ_0 , the incidence and azimuthal angles for exciting the XMD in non-misaligned samples, *i.e.* at $\mathbf{k}_0 = \mathbf{k}(\omega_0, \phi_0)$. Any reciprocal vector \mathbf{G} can also be written in terms of \mathbf{G}^0 , its position in non-misaligned samples, and a rotation matrix R as $\mathbf{G} = \mathbf{G}^0 R$. Then, by using Eq. (4) into Eqs. (2) and (3), $\Delta\omega$ and $\Delta\phi$ are determined by solving the following system of linear

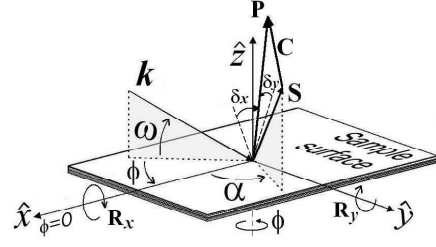


FIG. 1: Three-beam X-ray diffraction in misaligned crystals where the primary diffraction vector \mathbf{P} is not perfectly aligned along the azimuthal scanning axis (ϕ axis). The rotation matrices $R_x(\delta_x)$ and $R_y(\delta_y)$ account for the misalignment of the secondary and coupling diffraction vectors with respect to the $(\hat{x}, \hat{y}, \hat{z})$ goniometer reference system. \mathbf{k} is the wavevector of the incident radiation.

equations²⁴:

$$\begin{bmatrix} \mathbf{k}_\omega \cdot \mathbf{S} & \mathbf{k}_\phi \cdot \mathbf{S} \\ \mathbf{k}_\omega \cdot \mathbf{C} & \mathbf{k}_\phi \cdot \mathbf{C} \end{bmatrix} \begin{bmatrix} \Delta\omega \\ \Delta\phi \end{bmatrix} = - \begin{bmatrix} (\mathbf{S}/2 + \mathbf{k}_0) \cdot \mathbf{S} \\ (\mathbf{C}/2 + \mathbf{S} + \mathbf{k}_0) \cdot \mathbf{C} \end{bmatrix}. \quad (5)$$

A common reference system is required to describe all vectors in the above equations. Here, the $(\hat{x}, \hat{y}, \hat{z})$ goniometer system shown in Fig. 1 will be used. \hat{z} is along the ϕ axis, and \hat{x} is an arbitrary reference direction chosen for $\phi = 0$. For sake of simplicity, the vectors are represented by the 1×3 matrices of their components, for instance

$$\mathbf{k} = -\lambda^{-1}(\cos\omega \cos\phi, \cos\omega \sin\phi, \sin\omega), \quad (6a)$$

$$\mathbf{k}_\omega = -\lambda^{-1}(-\sin\omega_0 \cos\phi_0, -\sin\omega_0 \sin\phi_0, \cos\omega_0), \quad (6b)$$

$$\mathbf{k}_\phi = -\lambda^{-1}(-\cos\omega_0 \sin\phi_0, \cos\omega_0 \cos\phi_0, 0), \quad (6c)$$

and

$$\mathbf{G}^0 = (G_x, G_y, G_z). \quad (6d)$$

A general sample misalignment is taken into account by two rotation matrices $R_x(\delta_x)$ and $R_y(\delta_y)$ around the \hat{x} and \hat{y} directions (Fig. 1), and the total sample misalignment, for $\delta_{x,y} \ll 1$, is

$$R = R_y R_x \approx R_x R_y \approx \begin{bmatrix} 1 & 0 & -\delta_y \\ 0 & 1 & -\delta_x \\ \delta_y & \delta_x & 1 \end{bmatrix}. \quad (7)$$

Therefore,

$$\Delta \mathbf{G} = \mathbf{G} - \mathbf{G}^0 = (G_z \delta_y, G_z \delta_x, -G_x \delta_y - G_y \delta_x) \quad (8)$$

corresponds to the displacement of any diffraction vector due to crystal misalignment.

The incident beam direction for non-misaligned samples $\mathbf{k}_0 = \mathbf{k}(\omega_0, \phi_0)$ is calculated by Eqs. (1) and (2), which provide ω_0 and ϕ_0 since

$$\sin \omega_0 = \lambda |\mathbf{P}|^2 / 2 \quad (9a)$$

and

$$\cos(\phi_0 - \alpha) = \cos \beta = \frac{\lambda |\mathbf{S}|^2 / 2 - S_z \sin \omega_0}{S_{xy} \cos \omega_0}. \quad (9b)$$

where $\mathbf{S}_x = \mathbf{S}_{xy} \cos \alpha = \hat{x} \cdot \mathbf{S}^0$ and $\mathbf{S}_y = \mathbf{S}_{xy} \sin \alpha = \hat{y} \cdot \mathbf{S}^0$.

According to Eq. (9b) there are two azimuthal positions, commonly called 'out-in' and 'in-out', where the same secondary reflection is excited: $\phi_1 = \alpha - \beta$ and $\phi_2 = \alpha + \beta$. Precise lattice-parameter determination procedures are based on the experimental measurements of both positions. They provide $2\beta_{exp} = \phi_{2,exp} - \phi_{1,exp}$ for the calculation of the unit cell parameters from Eqs. (9), as described elsewhere (see for instance reference²⁰). The sample misalignment is measured by rocking curves of the primary reflection at $\phi = 0, 90^\circ, 180^\circ$, and 270° . If $\omega_0, \omega_{90}, \omega_{180}$ and ω_{270} are the respective rocking curves peak positions,

$$\delta_x = (\omega_{270} - \omega_{90})/2 \quad \text{and} \quad \delta_y = (\omega_{180} - \omega_0)/2. \quad (10)$$

The $\Delta\phi_n$ corrections in the 'out-in' ($n = 1$) and 'in-out' ($n = 2$) azimuthal positions are then obtained from Eq. (5), and they can be used either to refine the $2\beta_{exp}$ value according to

$$2\beta_{exp} = (\phi_{2,exp} - \Delta\phi_2) - (\phi_{1,exp} - \Delta\phi_1) \quad (11)$$

or to estimate misalignment effects on different secondary reflections, for instance those providing some useful information about the crystalline structure of the sample. To demonstrate this in practice, the in-plane strain of a GaAs (001) substrate induced by InAs quantum dots (QDs) is inspected in the following sections of this article.

III. EXPERIMENTAL

Data collection has been carried out at the Brazilian Synchrotron Light Laboratory (LNLS) D12A (XRD-1) beam-line, with the polarimeter-like diffractometer²⁵. The smallest step size is 0.0004° in both ω and ϕ axes. The

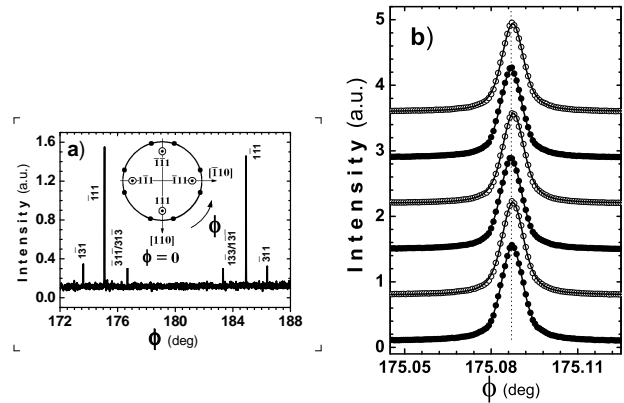


FIG. 2: (a) Renninger scans of the 002 GaAs reflection carried out with X-ray wavelength $\lambda = 1.330234\text{\AA}$. The highest peaks at 175.08° and 184.92° correspond to the excitation of the $\bar{1}\bar{1}1$ ('in-out') and $1\bar{1}\bar{1}$ ('out-in') secondary reflections, respectively. The others secondary reflections shown in the diagram are also indexed. In the inset, $[110]$ is the reference direction, $\phi = 0$, and the vectors corresponding to the $[111]$, $[\bar{1}\bar{1}1]$, $[\bar{1}\bar{1}\bar{1}]$, and $[1\bar{1}\bar{1}]$ directions are pointing outward the paper. The eight closed circles symbols indicate the azimuthal ϕ positions of all secondary reflections and their values are shown in Table 1. (b) Several high-resolutions ϕ scans measured around $\phi = 175.08^\circ$ position (solid circle) and after a 360° ϕ rotation (open circles). The peak positions have been determined by fitting the experimental intensity curves (open/solid circles) with lorentzian-gaussian convolution curves (solid lines), as explained in the text. The maximum shift observed in the peak position is $\phi_{max} - \phi_{min} = 0.00075^\circ$.

wavelength value, $\lambda = 1.330234\text{\AA}$ from a Si (111) double-crystal monochromator, was measured by rocking curves the 111 and 333 Silicon reflections. The incidence plane was set to the vertical position, scattering upwards (σ -polarization). The sample used in this study is a commercial GaAs (001) substrate with InAs quantum dots (QD) grown by molecular beam epitaxy (MBE) using a rate of 0.009 monolayer per second (mL/s). A 300\AA thick GaAs cap layer was grown on top of the QDs.

IV. RESULTS AND DISCUSSIONS

Table I shows the 'out-in' (ϕ_1) and 'in-out' (ϕ_2) azimuthal XMD peaks positions for the 111, $\bar{1}\bar{1}1$, $\bar{1}\bar{1}\bar{1}$, and $1\bar{1}\bar{1}$ secondary reflections in the Renninger scanning of the 002 GaAs reflection. The peak positions were determined by fitting the intensity data with lorentzian-gaussian convolution curves: a lorentzian standing for the intensity profile (FWHM = 0.0048°) of the peaks while the instrumental broadening was taken into account by a gaussian function (FWHM = 0.0060°). A short portion of the Renninger scan, around $\phi = 180^\circ$, is shown in Fig. 2a; the $[110]$ direction was taken as reference for

$\phi = 0$. To assure that the data are free of instrumental errors, the ϕ scan of a chosen XMD peak, in this case the peak at $\phi = 175.08^\circ$, was repeated after measuring the other peaks without changing the ϕ axis rotation sense, *i.e.* after a 360° ϕ rotation, see Fig.(2)b. Each ϕ scan has been performed at the (002) rocking-curve maximum which was carried out about 0.5° before the XMD peak positions.

The rocking curves used to characterize the sample misalignment are shown in Fig. 3; they provide $\delta_x \simeq 0.0009^\circ$ and $\delta_y \simeq 0.0067^\circ$. However, in general, for small sample misalignments Eq. (5) can be linearized by numerical derivation, and the corrections of the XMD ϕ positions can be written as $\Delta\phi_n = A_n\delta_x + B_n\delta_y$. For the particular set of secondary reflections investigated here, the values of A_n and B_n coefficients are given in Table I (last two rows). By replacing these values into Eq. (11), it is possible to demonstrate that

$$\bar{\beta}_{[110]} = (\beta_{111} + \beta_{\bar{1}\bar{1}\bar{1}})/2 \quad (12a)$$

and

$$\bar{\beta}_{[\bar{1}\bar{1}0]} = (\beta_{\bar{1}\bar{1}\bar{1}} + \beta_{111})/2 \quad (12b)$$

do not depend on δ_x and δ_y . In other words, the average β_{exp} for the secondary reflections with in-plane components in the [110] and $[\bar{1}\bar{1}0]$ orthogonal directions, $\bar{\beta}_{[110]}$ and $\bar{\beta}_{[\bar{1}\bar{1}0]}$, are misalignment-free experimental values, and therefore, very useful for precise lattice parameter measurements in both orthogonal directions.

We assume a tetragonal lattice distortion where the substrate in-plane lattice parameter is given by $a = b = (1 - \nu)a_0$ while, to preserve the unit cell volume, $c = (1 + 2\nu)a_0$. For $a_0 = 5.6534\text{\AA}$, $|\mathbf{P}| = 2/c$, $\mathbf{S}^0 = (h/a, k/b, 1/c)$ (in the crystal reciprocal space) and $h, k = \pm 1$, Eq. (9) provides

$$\beta(\nu) = 85.08984^\circ - 33.85^\circ\nu. \quad (13)$$

Note that $|\mathbf{S}| = |\mathbf{S}^0|$ is invariant under any rotation, but their components are not. Therefore, S_x , S_y and S_z in Eq. (9b) must be calculated for $\hat{x} = (1, 1, 0)/\sqrt{2}$, $\hat{y} = (\bar{1}, 1, 0)/\sqrt{2}$ and $\hat{z} = (0, 0, 1)$, *i.e.*, $S_x = (h+k)/(a\sqrt{2})$, $S_y = (-h+k)/(a\sqrt{2})$ and $S_z = 1/c$.

In the 002 Renninger scan of (001) samples, $hk1$ secondary reflections give rise to special XMD cases, named Bragg-surface diffractions, where the secondary-beam directions are very close to surface in-plane directions. The extreme asymmetry of such secondary reflections limits the secondary wavefield penetration depth to less than $1\ \mu\text{m}$. Experimentally, this value has been measured by reciprocal-space mapping of the 002 rod in GaAs (001) crystals undergoing Bragg-surface diffraction. It has been demonstrated that about 80% of the diffraction intensity, for X-ray photons of 8 keV, is attenuated in the

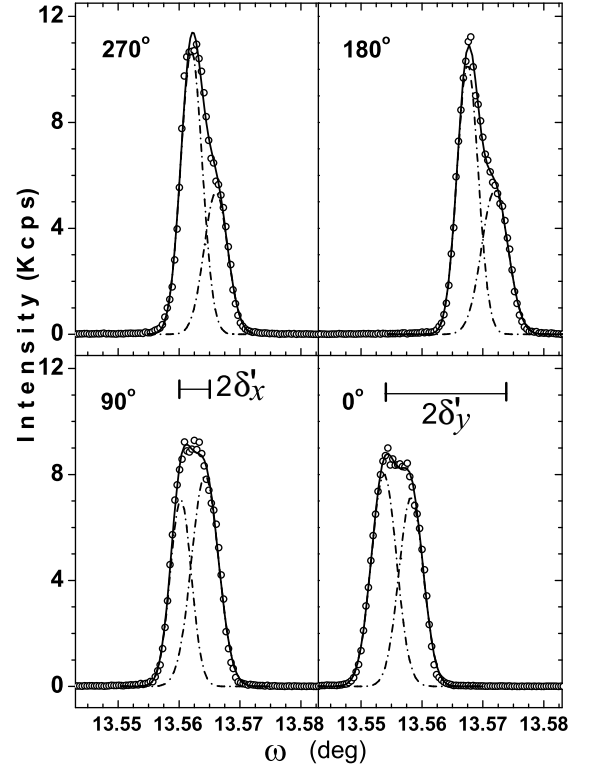


FIG. 3: Experimental (open circles) and simulated (solid lines) rocking curves, ω -scans, of the 002 primary reflection measured at $\phi = 0, 90^\circ, 180^\circ$ and 270° , as shown aside of each scan. These scans were simulated by using two gaussian curves (dashed lines) whose splitting is about $\Delta\omega = -0.00422(24)^\circ$. It provides $\Delta c/c = 3.0(2) \times 10^{-4}$. The misalignment angles calculated from the gaussians at lower ω values are $\delta_x \simeq 0.0009^\circ$ and $\delta_y \simeq 0.0069^\circ$, while $\delta'_x (= 0.0024^\circ)$ and $\delta'_y (= 0.0103^\circ)$ were obtained from the β values in Table I.

first $0.3\ \mu\text{m}$ below the surface²⁶. According to this fact, the observed tetragonal deformation would correspond to an average value of a shallow layer just below the surface where the induced strain due to the InAs QD is significant. Although the InAs epitaxial growth generates an expansive stress in the substrate lattice under the QDs, the adjacent regions are compressed as schematically illustrated in Fig. 4.

Differences in the tetragonal distortion along the [110] and $[\bar{1}\bar{1}0]$ directions, *i.e.* $\bar{\beta}_{[110]} \neq \bar{\beta}_{[\bar{1}\bar{1}0]}$, would yield a unit cell slightly twisted near the substrate surface. For instance, tiny variations in the γ angle, between the \mathbf{a} and \mathbf{b} lattice vectors, can be estimated by numerical derivation of Eq. (9). In this case, it leads to

$$\bar{\beta}_{[\bar{1}\bar{1}0]} - \bar{\beta}_{[110]} = (C_{\bar{1}10} - C_{110})\Delta\gamma \quad (14)$$

where $C_{\bar{1}10} = 0.1276$ and $C_{110} = -0.1302$, and then to $\gamma = 89.9985^\circ \pm 0.0018^\circ$.

TABLE I: Azimuthal positions of the 111, $\bar{1}\bar{1}\bar{1}$, $\bar{1}11$, and $1\bar{1}\bar{1}$ secondary reflections in the Renninger scanning of the 002 GaAs primary reflection. Each position was measured three times (rows 1, 2 and 3) as explained in the text, $\bar{\phi} = (\phi_{max} + \phi_{min})/2$, $\varepsilon = (\phi_{max} - \phi_{min})/2$, $\beta_{exp} = (\bar{\phi}_2 - \bar{\phi}_1)/2$, $\bar{\beta}$ are the average misalignment-free values, ν stands for the unit-cell tetragonal distortion (Eq. (13)) and $\beta_{mis} = \bar{\beta} + (\Delta\phi_2 - \Delta\phi_1)/2$ (Eq. (11)), where $\Delta\phi_n = A_n\delta'_x + B_n\delta'_y$, $\delta'_x = 0.0024^\circ$, and $\delta'_y = 0.0103^\circ$. A_n and B_n were estimated by numerical derivation of Eq. (5). Angular values are given in degrees.

	111		$\bar{1}\bar{1}\bar{1}$		$\bar{1}11$		$1\bar{1}\bar{1}$	
	ϕ_1	ϕ_2	ϕ_1	ϕ_2	ϕ_1	ϕ_2	ϕ_1	ϕ_2
1	-85.07750	85.08599	94.91867	265.09121	4.92085	175.08692	184.92072	355.08935
2	-85.07716	85.08575	94.91853	265.09141	4.92102	175.08688	184.92061	355.08881
3	-85.07683	85.08548	94.91819	265.09209	4.92105	175.08730	184.92064	355.08880
$\bar{\phi}$	-85.077165	85.085735	94.91843	265.09165	4.92095	175.08709	184.920665	355.089075
ε	± 0.000335	± 0.000255	± 0.00024	± 0.00044	± 0.00010	± 0.00021	± 0.000055	± 0.000275
β_{exp}	85.081450 \pm 0.000295		85.08661 \pm 0.00034		85.083070 \pm 0.000155		85.084205 \pm 0.000165	
$\bar{\beta}$	85.08403 \pm 0.00032				85.08364 \pm 0.00016			
ν	$(1.716 \pm 0.096) \times 10^{-4}$				$(1.832 \pm 0.048) \times 10^{-4}$			
β_{mis}	85.0815		85.0865		85.0831		85.0842	
A_n	0.0207	0.0207	-0.0207	-0.0207	0.2412	-0.2412	-0.2413	0.2413
B_n	0.2412	-0.2412	-0.2413	0.2413	-0.0207	-0.0207	0.0207	0.0207

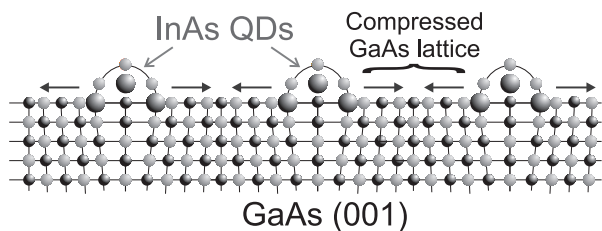


FIG. 4: Schematic illustration of the compressive stress generated by InAs QDs on GaAs substrate. There is also a 300Å thick GaAs cap layer over the QDs (not shown in the figure).

Finally, the agreement between the δ_x and δ_y and δ'_x and δ'_y values is better when rocking curves are measured with higher definition in their maximum peak position.

V. CONCLUSIONS

In summary, a method that corrects any sample misalignment and allows the determination of highly accurate single-crystals lattice parameters or their variation was presented. The advantage of this method is in the measurement of rocking curves in orthogonal positions. By combining those rocking curves and measurements of a XMD secondary reflection family, having the same β value and measured in their "in-out" and "out-in" azimuthal positions, the effects of a residual sam-

ple misalignment is eliminated and any systematic error is averaged out. Therefore, a precision better than $1/10000\text{\AA}$ can be easily achieved.

As the method presented here can determine very small single crystal lattice deformations, it is an excellent tool for studying epitaxial nanostructures grown on top of crystalline substrates. The strain field produced by the nanostructures in the substrate lattice can be determined even when those nanostructures are buried by cap layers. As an application, QDs grown on GaAs (001) were analyzed and the results showed that the GaAs lattice is tetragonally distorted and slightly twisted near the substrate surface.

The method however, is not restricted to the particular geometry of the QDs system studied in this work where, due to the primary diffraction vector high symmetry, a family of eight secondary reflections could be measured. When the system symmetry under study is lower, it is only important to obtain rocking-curves profiles with well-defined peak positions.

Acknowledgments

This work was supported by the Brazilian funding agencies FAPESP (grant numbers 02/10185-3 and 02/10387-5), CNPq (proc. number 301617/95-3 and 150144/03-2) and LNLS (under proposal number D12A-XRD1 2490/03).

* Electronic address: lhavanci@if.usp.br

† Electronic address: rocha@fisica.ufc.br

‡ Electronic address: aquivy@macbeth.if.usp.br

§ Electronic address: morelhao@if.usp.br

¹ S. L. Morelhão and L. P. Cardoso, J. Appl. Cryst. **29**(4), 446-456 (1996).

² M. A. Hayashi, S. L. Morelhão, L. H. Avanci, L. P. Car-

- doso, J. M. Sasaki, L. C. Kretly and S.-L. Chang, *Appl. Phys. Lett.* **71**(18), 2614-2616 (1997).
- ³ L. H. Avanci, L. P. Cardoso, S. E. Girdwood, D. Pugh, J. N. Sherwood and K. J. Roberts, *Phys. Rev. Lett.* **81**, 5426-5429 (1998).
- ⁴ L. H. Avanci, L. P. Cardoso, J. M. Sasaki, S. E. Girdwood, K. J. Roberts, D. Pugh and J. N. Sherwood, *Phys. Rev. B* **61**, 6507-6514 (2000).
- ⁵ J. M. A. Almeida, M. A. R. Miranda, C. M. R. Remédios, F. E. A. Melo, P. T. C. Freire, J. M. Sasaki, L. P. Cardoso, A. O. dos Santos and S. Kycia, *J. Appl. Cryst.* **36**(6), 1348-1351 (2003).
- ⁶ A. O. dos Santos, L. P. Cardoso, J. M. Sasaki, M. A. R. Miranda and F. E. A. Melo, *J. Phys.-Condensed Matter* **15**(46), 7835-7842 (2003).
- ⁷ X. Lai, K. J. Roberts, L. H. Avanci, L. P. Cardoso and J. M. Sasaki, *J. Appl. Cryst.* **36**(5), 1230-1235 (2003).
- ⁸ S.-L. Chang, *Appl. Phys. Lett.* **37**, 819-821 (1980).
- ⁹ R. Colella, *Acta Cryst. Sect. A* **30**, 413-423 (1974).
- ¹⁰ H. J. Juretschke, *Phys. Rev. Lett.* **48**, 1487-1489 (1982).
- ¹¹ S.-L. Chang, *Int. J. Mod. Phys. B* **6**, 2987-3020 (1992) and references therein.
- ¹² E. Weckert and K. Hmmer, *Acta Crystallogr. Sect. A* **53**, 108-143 (1997) and references therein.
- ¹³ S. L. Morelhão and S. Kycia, *Phys. Rev. Lett.* **89**(1), Art. No. 015501 (2002).
- ¹⁴ C.-H. Du, M.-T. Tang, Y. P. Stetsko, Y.-R. Lee, C.-W. Wang, C.-W. Cheng and S.-L. Chang, *Acta Cryst. A* **60**, 209-213 (2004).
- ¹⁵ Y. Zhang, R. Colella, Q. Shen and S. W. Kycia, *Acta Cryst. Section A* **54**(4), 411-415 (1998).
- ¹⁶ Q. Shen, S. Kycia and I. Dobrianov, *Acta Cryst. Section A* **56**(3), 268-279 (2000).
- ¹⁷ B. S. Fraenkel, *Appl. Phys. Lett.* **36**, 341-343 (1980).
- ¹⁸ B. S. Fraenkel, *Appl. Phys. Lett.* **41**, 234-236 (1982).
- ¹⁹ S. L. Morelhão and L. H. Avanci, *Acta Cryst. Section A* **57**(2), 192-196 (2001).
- ²⁰ B. Post, *J. Appl. Cryst.* **8**, 452-456 (1975).
- ²¹ T. Hom, W. Kiszewick and B. Post, *J. Appl. Cryst.* **8**, 457-458 (1975).
- ²² H. Cole, F. W. Chambers and H. M. Dunn, *Acta Cryst.* **15**, 138-144 (1962).
- ²³ S. Caticha Ellis, *Jpn. J. Appl. Phys.* **14**(5), 603-611 (1975).
- ²⁴ S. L. Morelhão, A. A. Quivy and J. Härtwig, *Microel. Journal* **34**, 695-699 (2003).
- ²⁵ S. L. Morelhão, *J. Sync. Rad.* **10**, 236-241 (2003).
- ²⁶ S. L. Morelhão and E. Abramof, *J. Appl. Cryst.* **33**, 871-877 (1999).